

Dissipative transport of thermalized electrons through a nanodevice

M. Wołoszyn and B. J. Spisak*

AGH University of Science and Technology, Faculty of Physics and Applied Computer Science, al. Mickiewicza 30, 30-059 Krakow, Poland

(Received 8 May 2017; revised manuscript received 16 June 2017; published 29 August 2017)

An equilibrium distribution function which corresponds to thermalization of electrons in contacts due to scattering processes is introduced for the purpose of reformulation of the inflow boundary conditions for the Wigner kinetic equation. The importance of the proposed concept for more realistic descriptions of transport phenomena in nanodevices is illustrated by determination of characteristics of the nanowire in cases of dissipative and dissipationless states of its active region. Quantitative results show how transport characteristics of the nanodevice are modified by the contacts.

DOI: [10.1103/PhysRevB.96.075440](https://doi.org/10.1103/PhysRevB.96.075440)

I. INTRODUCTION

Since realistic electronic nanodevices can be regarded as open quantum systems [1,2], it follows that they are usually intended to serve as basic building blocks of a larger electrical circuit. Hence, the importance of the proper description of the transport phenomena in the nanodevices, which on one hand should include the wavelike properties of the conduction electrons, but on the other hand should also cover the exchange of energy with environment and the exchange of carriers with the contacts. We may expect that the dynamics of electrons in the presence of an electric field will be determined by a nontrivial interplay between the quantum coherence of the carriers and scattering processes that destroy the phase coherence. One of the possible approaches that allows one to consider the loss of the electronic phase coherence in an elegant way employs the concept of the Wigner distribution function (WDF). The WDF is defined by the Weyl transform of the density matrix, $\rho(x, x')$, in the following way [3–6]: $f(x, k) = 1/(2\pi\hbar) \int dX \rho(x - X/2, x + X/2) \exp(-ikX)$. The side effect of this transformation is that WDF takes negative values in some regions of the phase space [7]. In turn, the Weyl transform converts the equation of motion for the density matrix to the form of the kinetic equation for the WDF, wherein the drift term has the nonlocal form [8].

Currently, the phase space approach to the quantum mechanics based on the WDF is an active field of research in different branches of modern physics [9–17]. It stems from the fact that this approach offers a slightly different point of view on description of quantum phenomena, and a relatively easy way to include the interaction with environment [18,19]. On the other hand, this method has been known for its applications to simulate the transport properties of nanodevices for many years, in particular because of the flexibility that makes it possible to include the scattering term within the relaxation time approximation [20,21]. The method still remains an attractive tool for research on the transport properties of the nanosystems, not free of some drawbacks, however, being rather technical than conceptual. Skillful analysis based on the physical arguments removes the difficulties [22–24].

Recently, considerable effort has been devoted to improving the numerical methods of solving the quantum kinetic equation

for the WDF. The stochastic methods based on different variants of the Monte Carlo techniques [8,25–27] seem to be very promising for the computational nanoelectronics since they allow for the computer simulations of multidimensional nanosystems, including the effects of the many electron interactions. Combinations of Gaussian wave packets entering an active region of a nanodevice from opposite sides have been considered [28], and efficient numerical schemes based on the nonuniform meshes are still developed for the deterministic discretization methods [29–32]. Moreover, the fast Fourier transform is also used to solve the equation for the WDF in the Moyal form via the split-operator method [33–36].

In this paper, we propose the boundary conditions based on the equilibrium distribution functions corresponding to thermalization of electrons due to scattering processes taking place in these parts of nanodevices that are out of scope of simulation's active region. Motivation for our proposal arises out of some hints presented by numerous authors in the context of generalization of the Landauer current formula, e.g., in Refs. [37–39]. Furthermore, fabrication of high-quality contacts, which are not spatially inhomogeneous nor defected, is a serious experimental problem [40,41].

Presented results shed some light on the theoretical description and methods of simulation, taking into account the quality of contacts and their influence on the transport characteristics of nanodevices. For this purpose, we consider a semiconductor nanowire containing a double-barrier structure, since the systems of that kind are the subject of many experiments using various semiconductor materials [42–45]. Based on the results of Refs. [46,47], we assume that the description of this system can be reduced to an effectively one-dimensional model of the nanodevice. This simplification allows us to directly apply the Wigner kinetic equation with the phenomenological dissipative term to examine the influence of the proposed boundary conditions. The obtained results clearly prove that the investigated effect of thermalization strongly reduces the electronic current through the nanowire, regardless of the dissipative flow of conduction electrons included in the kinetic equation.

This paper is organized as follows: In Sec. II we present and discuss the proposed modification of the boundary conditions for the Wigner equation and present a model of the semiconductor nanowire to which we apply those conditions. Section III contains the results of calculations, their discussion, and further generalization. Finally, Sec. IV contains conclusions and summary of the results.

*bjs@agh.edu.pl

II. THEORY

In many cases, when we think about conduction electrons which are injected into a nanosystem, we assume that they are described by the plane waves, i.e., we apply the free electron model in which the distribution of electronic states is described by the Fermi-Dirac distribution function [48]

$$f^{L(R)}(E(k)) = \frac{1}{\exp\left[\frac{E(k) - \mu_{L(R)}}{k_B T}\right] + 1}, \quad (1)$$

where $E(k) = \hbar k^2/2m^*$ is the quadratic dispersion relation, T is the temperature, $\mu_{L(R)}$ is the electrochemical potential in the left (right) contact, and the rest of symbols have their usual meaning. This line of thinking can bring about the boundary conditions that assume that the states of conduction electrons flowing into the nanosystem depend on the states of the contacts as follows [20]:

$$\begin{aligned} f(x=0, k)|_{k>0} &= f^L(E(k)), \\ f(x=L, k)|_{k<0} &= f^R(E(k)), \end{aligned} \quad (2)$$

where $f^{L(R)}(E(k))$ are the Fermi-Dirac functions for the left (L) and right (R) contacts. The logic of this approach leads to the artificial spatial separation between the nanosystem and the contacts, which is inconsistent with the nonlocal character of the quantum mechanics and sometimes may produce unphysical results, as was pointed out in Refs. [23, 49]. One possible way to overcome these difficulties is to include the interaction of the carriers with phonons and impurities in the considered nanodevices, which diminishes the effect of the interfaces [50]. This idea can be realized by averaging the Fermi-Dirac function over the energy, with a weight function that depends on those processes via the appropriate relaxation times [51]. The resulting distribution function guarantees thermal equilibrium for the conduction electrons [52].

According to the above statement, we modify the standard inflow boundary conditions [Eq. (2)] in such way that the scattering processes in contacts are also included. To achieve this, we replace the Fermi-Dirac function with its convolution with the broadened Dirac delta $\delta_\Gamma(E)$, namely [51–53]

$$f_{\text{eq}}^{L(R)}(E(k)) = \int_0^\infty dE \delta_\Gamma(E - E(k)) f^{L(R)}(E), \quad (3)$$

where $\delta_\Gamma(E)$ is represented by a Γ -parametrized Lorentzian-shape function with a width proportional to the phase-breaking strength Γ (see Appendix for more details on the choice of Lorentzian),

$$\delta_\Gamma(E - E(k)) = \frac{1}{\pi} \frac{\Gamma}{[E - E(k)]^2 + \Gamma^2}. \quad (4)$$

We note that the standard form of the distribution function given by Eq. (1) is recovered from Eq. (3) in the limit of $\Gamma \rightarrow 0$. Then, the sequence of the functions given by Eq. (4) is replaced by the Dirac delta distribution that can be regarded as a spectral weight function for the free electron gas [51], which, in principle, justifies our strategy. In general, a finite value of Γ may be due to the energy exchange between interacting electrons, the interaction between electrons and phonons, or other scattering processes. For the purpose of this study, we define the parameter Γ as the imaginary part of the

self-energy Σ . Calculating the self-energy is a complex task and it depends on the details of the electronic structure, but for simplicity we assume that the one-particle electronic quantities are smooth functions. Hence, the lowest order of the Born approximation in the scattering is a reasonable approximation for the present consideration of the self-energy. Within the simplest approximation we can write the relation between the imaginary part of the self-energy and the relaxation time as

$$\Gamma = -\Im \Sigma = \frac{\hbar}{2\tau_\Gamma}, \quad (5)$$

where τ_Γ is the relaxation time for the scattering processes included in the equilibrium distribution [Eq. (3)] [51].

To investigate the impact of the reformulated boundary conditions on the transport characteristics of the considered nanodevice, we solve the Wigner kinetic equation with the dissipative term which is modeled within the relaxation time approximation. This approach is fully justified in relation to the considered nanodevice [54], therefore the Wigner kinetic equation can be written in the form

$$\begin{aligned} \frac{\hbar k}{m^*} \frac{\partial f(x, k)}{\partial x} + \frac{1}{2\pi i \hbar} \int dk' W(x, k - k') f(x, k') \\ = -\frac{f(x, k) - f^0(x, k)}{\tau}, \end{aligned} \quad (6)$$

where $f^0(x, k)$ is the equilibrium WDF, τ is the relaxation time related to the scattering processes taking place in the active region of the nanodevice, and the integral kernel $W(x, k)$ is given by the formula

$$W(x, k) = \int d\xi \left[U\left(x + \frac{\xi}{2}\right) - U\left(x - \frac{\xi}{2}\right) \right] e^{-ik\xi}, \quad (7)$$

where $U(x)$ is the total potential energy of the conduction electron. For the present calculations, $U(x)$ consists of the sum of two terms, namely

$$U(x) = U_{cb}(x) + U_{el}(x). \quad (8)$$

The term $U_{cb}(x)$ results from the discontinuity of the conduction band, while $U_{el}(x)$ includes the potential energy due to the bias voltage V applied between the left and the right contact.

Equation (6) is solved numerically on the computational grid with $N_x = 133$ mesh points for the space coordinate x , and $N_k = 150$ points for the wave vector k , chosen accordingly to the restrictions on the minimum momentum resolution imposed by the uncertainty principle [31]. In the first step, the drift and diffusion terms in the Wigner equation are discretized [20] while the scattering term on the right-hand side of Eq. (6) is neglected. The application of the proposed boundary conditions leads then to a system of linear equations given by $N_x^2 \times N_k^2$ matrix, which is solved to find the values of $f^0(x, k)$ at all points of the computational grid. In the next step, the equation must be discretized once more, this time including the scattering term, to find the WDF $f(x, k)$. The whole procedure is then repeated for all required values of the applied bias voltage and relaxation times τ and τ_Γ .

The calculations that demonstrate the impact of the proposed generalization were performed for a nanowire of length $L = 75$ nm with embedded GaAs/AlGaAs double-barrier structure. Figure 1 shows the schematic and the

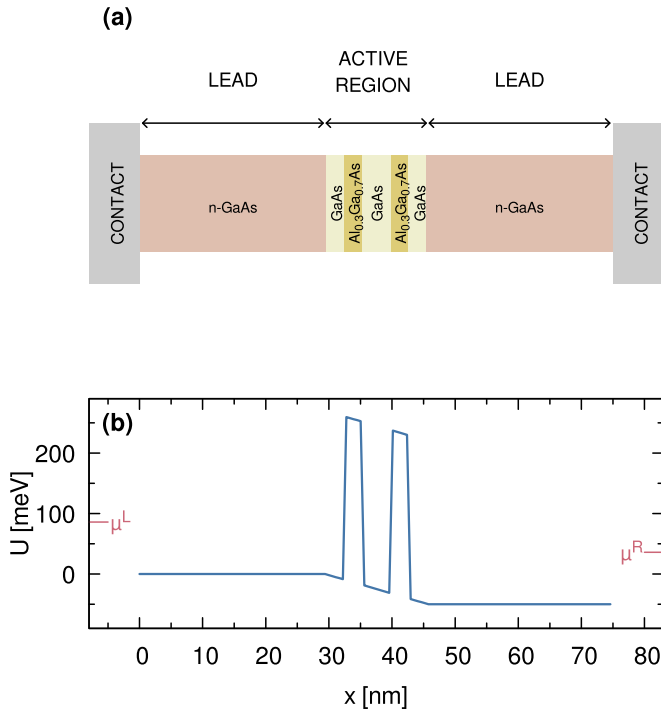


FIG. 1. (a) Schematic of the nanowire with active region containing embedded GaAs/Al_{0.3}Ga_{0.7}As double-barrier structure. (b) Potential energy profile along the axis of the nanowire resulting from the conduction band discontinuity, and for the applied bias voltage $V = 50$ mV.

potential energy profile along the axis of the nanodevice. The active region of the nanowire consists of two Al_{0.3}Ga_{0.7}As barriers surrounded by the GaAs spacers and separated by the GaAs quantum well. The simulation region also includes the n -GaAs leads, which are prone to nonuniform doping during the fabrication process [55]. The width of each of the barriers is 2.8 nm, the same as for the leads, and the well's width is 4.5 nm.

The effect of the adopted boundary condition is that the magnitude of the WDF at the boundaries of the contacts is reduced when compared to the standard boundary condition, i.e., to the case of $\Gamma = 0$, as illustrated in Fig. 2 by the example of the WDF calculated for the bias voltage matching the peak in the current-voltage characteristics. It shows that the scattering processes reduce the magnitude of the WDF at the boundaries, in particular for small k .

III. RESULTS AND DISCUSSION

The results of the calculations that are presented below were obtained for the temperature $T = 77$ K and for the electrochemical potential in the contacts equal to 86 meV. The height of each of the two Al_{0.3}Ga_{0.7}As barriers is 0.27 eV, and because of their relatively small width constant effective mass of GaAs, $m^* = 0.067m_0$, is assumed for the whole device (m_0 is the free electron mass).

A solution of the Wigner kinetic Eq. (6) allows determining the WDF for a given value of the applied bias voltage V related to the boundary condition. Then the electronic current, I , as a function of the bias voltage is calculated as a first moment of

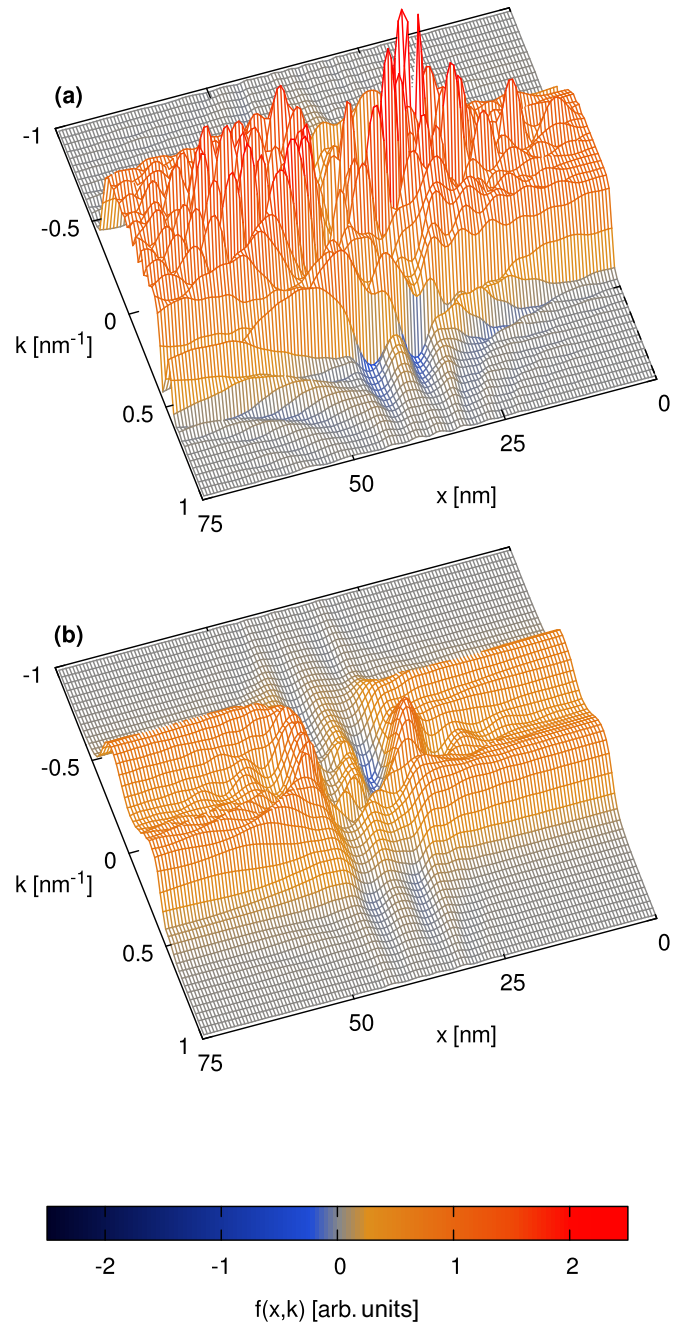


FIG. 2. The Wigner distribution function calculated for the bias voltage corresponding to the peak of the current, (a) without scattering and (b) for scattering times $\tau_\Gamma = 15$ fs and $\tau = 50$ fs.

the WDF in accordance to the formula

$$I(V) = \frac{e}{2\pi} \frac{1}{L} \int_0^L dx \int dk \frac{\hbar k}{m^*} f(x, k; V). \quad (9)$$

This calculation scheme is used to investigate the influence of electron's thermalization effect on the current-voltage characteristics of the nanodevice. The shape of this characteristic exhibits a peak that is a result of resonant tunneling through the double-barrier structure [56,57], as shown in Fig. 3(a). The position and width of this peak depend on the geometrical and material parameters of the resonant structure in the active

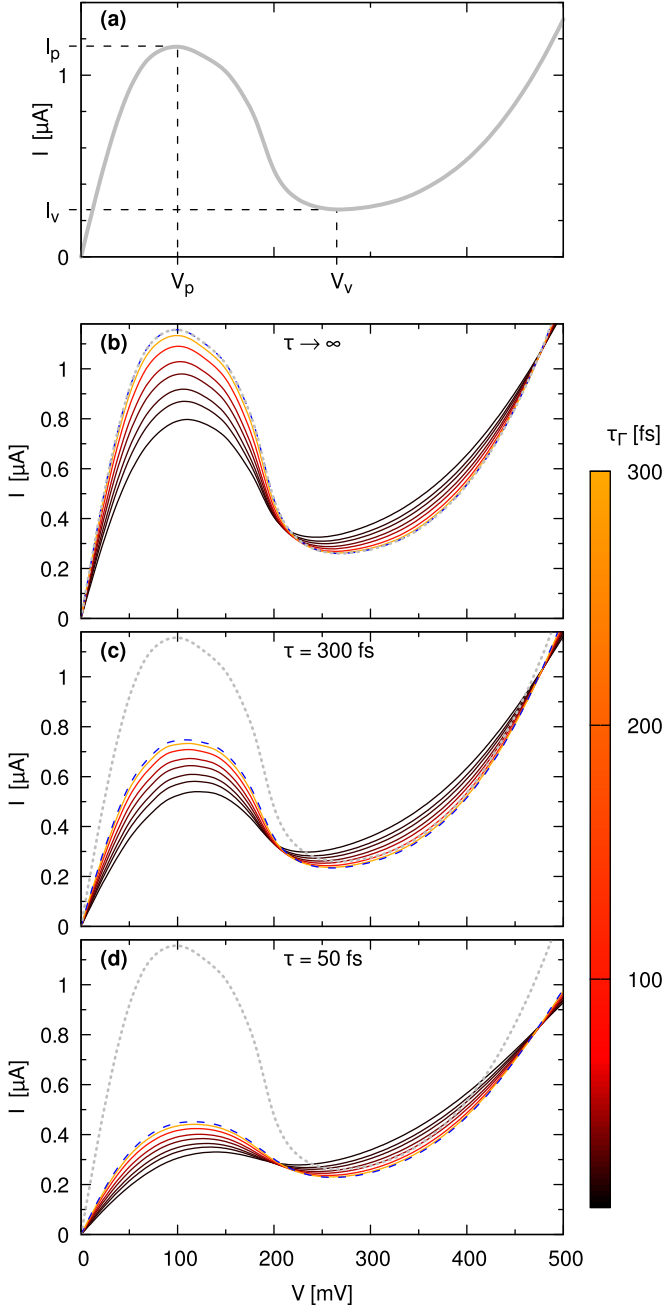


FIG. 3. (a) Current-voltage characteristics of the nanowire obtained when no scattering processes of any kind are included, and illustrating the definitions of the peak (valley) voltages, $V_{p(v)}$, and currents, $I_{p(v)}$. The characteristics calculated for varying relaxation time, τ_Γ , corresponding to the scattering processes in the contacts, is presented in (b) for the case without scattering inside the nanodevice, (c) For $\tau = 300$ fs, and (d) for $\tau = 50$ fs. In (b), (c), and (d), the blue dashed line shows the current for $\Gamma = 0$, while the gray dotted line indicates, for comparison, the characteristics shown in (a).

region. In order to show the significance of the proposed distribution function [cf. Eq. (3)] for the boundary conditions and thereby its effect on the transport characteristics, we have examined two operating regimes of the nanodevice.

In the first case, the active region of the nanowire and the leads are treated as dissipationless parts of the nanodevice.

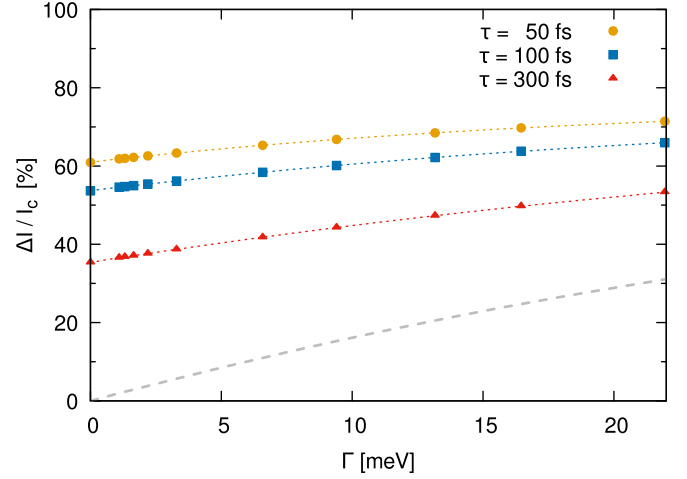


FIG. 4. Relative change of the peak current as a function of the parameter Γ for $\tau = 50, 100, 300$ fs. The dashed gray line corresponds to the case without scattering inside the nanowire.

Current-voltage characteristics for such a device were obtained from Eq. (9), with the WDF, which is the solution of Eq. (6) when the dissipation term is neglected. The results are presented in Fig. 3(b). The dotted line corresponds to the current values calculated with the boundary condition [Eq. (2)] generated using the bare Fermi-Dirac distribution function, which corresponds to the free electrons model. Analysis of the results obtained for the considered range of the parameter τ_Γ reveal that when thermalization effects are taken into account, the peak value of the current is up to 35% smaller than for the case of free electrons. It shows that thermalization of electrons in the contacts cannot be neglected because the considered effect is relatively significant.

In the second case, we have analyzed the changes of current-voltage characteristics when dissipation inside the nanowire is included. The range of the used relaxation times is estimated with respect to the effective value of mobility in GaAs, $\mu = e\tau/m^*$. Solution of Eq. (6) for this case leads to the results presented in Figs. 3(c) and 3(d), which also show values obtained when no scattering in the nanodevice or in the contacts is taken into account (gray dotted line). Based on those relations, we may conclude that scattering of the thermalized electrons significantly affects the current-voltage characteristics. For example, when $\tau = 300$ fs, the peak value of current is reduced by ca. 60% compared to the coherent current of free electrons, and up to 70% when thermalization of electrons is considered with $\tau_\Gamma = 20$ fs. For shorter relaxation time, $\tau = 50$ fs, those changes are smaller, about 35% and 55%, correspondingly. A more detailed investigation of those effects is possible based on the values of the relative change of peak current, according to the formula

$$\frac{\Delta I}{I_c} = \frac{I_c - I(\Gamma)}{I_c}, \quad (10)$$

where I_c is the current of the dissipationless flow of free electrons [58]. Figure 4 shows $\Delta I/I_c$ calculated for the peak current as a function of intensity of scattering.

This result demonstrates that contribution of the thermalization of electrons in the contacts leads to the 10-20% change

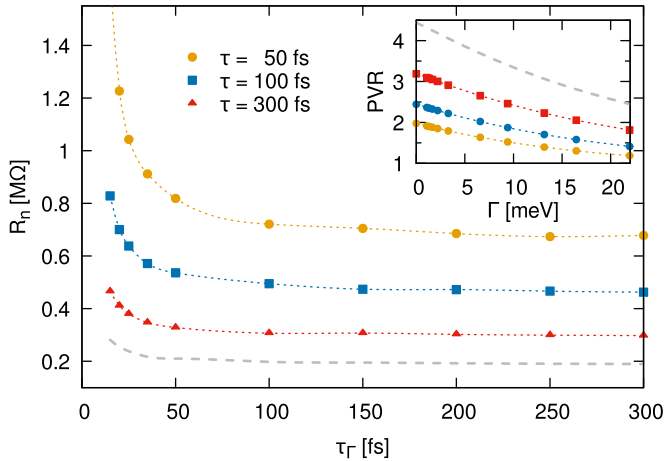


FIG. 5. The absolute value of the negative resistance R_n for $\tau = 50, 100, 300$ fs, and for the case when no scattering inside the nanowire is assumed (dashed gray line). The inset shows the peak-to-valley ratio (PVR) as a function of the parameter Γ .

of the current, depending on the intensity of dissipation in the nanowire. It proves that the transport properties of real nanodevices depend not only on the quality of the active region (in this case, inside a nanowire), but also on the quality of contacts influenced by various scattering processes resulting in thermalization of conduction electrons.

The above analysis can be extended into another transport characteristic of the nanodevice [59]. In particular, we inspect the influence of the thermalization effect on the negative resistance which is defined as

$$R_n = \frac{V_v - V_p}{I_p - I_v}, \quad (11)$$

where V_p and V_v are the peak and valley voltages, while I_p and I_v are the corresponding peak and valley currents [cf. Fig. 3(a)], found separately for different relaxation times. As it follows from the results shown in Fig. 5, the negative resistance for short relaxation times τ_r , up to about 50 fs, decreases with increasing τ_r , while for longer times it remains approximately constant. Independently of the negative resistance, we perform analysis of the peak-to-valley ratio (PVR) which is another figure of merit used to characterize the current-voltage characteristics. In this case PVR decreases as a function of increasing Γ in the whole range of the values used in our calculations (see the inset of Fig. 5). When compared to the value obtained without scattering, PVR decreases by about 45% when $\tau = 100$ fs (but without scattering in contacts), and by 70% when additionally $\tau_r = 20$ fs is assumed.

The presented results can be further generalized if the momentum- and energy-dependence of the relaxation time is considered, which leads to the self-consistent calculations of the relaxation time derived within the Wigner formalism [60]

$$\tau_r^{-1}(\mathbf{k}, \omega) = \frac{2\pi}{\hbar} \frac{1}{\Omega} \sum_{\mathbf{k}'} n_I |M(\mathbf{k}', \mathbf{k}; \omega)|^2 \times \frac{\hbar \tau_r^{-1} \left(\frac{\mathbf{k} + \mathbf{k}'}{2} \right)}{\pi \left\{ [E(k) - E(k') + \hbar\omega]^2 + \left[\hbar \tau_r^{-1} \left(\frac{\mathbf{k} + \mathbf{k}'}{2} \right) \right]^2 \right\}}, \quad (12)$$

where $M(\mathbf{k}', \mathbf{k}; \omega)$ is the transition matrix element due to quasielastic or inelastic scattering processes ($\omega = 0$ corresponds to a purely elastic scattering), and n_I is the concentration of scattering centers in the contact having volume Ω . It is interesting to note that the inverse of the relaxation time given by Eq. (12) is proportional to the product of the transition matrix element and broadened Dirac delta, provided that we neglect its momentum dependence.

IV. CONCLUSIONS

We have reformulated the inflow boundary conditions which are commonly used for the description of the transport properties of the nanodevices by means of the Wigner equation or Wigner-Poisson approach. For this purpose, we have used the equilibrium distribution function, which is defined as the convolution of the Fermi-Dirac distribution with the spectral weight function, instead of the bare Fermi-Dirac distribution function for the free electrons model. Owing to that, it is possible to take into consideration the scattering processes in these parts of nanodevices, which are outside the simulated region.

We have tested the influence of the proposed boundary condition on the transport characteristics of the nanodevice in which the active region consists of a double-barrier structure embedded in a nanowire. We have performed the calculations in two transport regimes. In the first case, we have assumed that transport through the active region and leads is dissipationless, while in the second case it is dissipative. The latter has been achieved by including the scattering integral to the Wigner equation and modeling it within the relaxation time approximation.

Our calculations show how transport characteristics, i.e., the current-voltage dependence, the negative resistance, or peak-to-valley ratio, are modified when the scattering processes are included, in comparison to the calculations conducted without any type of scattering taken into account, or only with inclusion of the scattering processes in the active region of the nanodevice. We have found that the expected decrease of the peak current due to the thermalization effects can be estimated to be about 10-20%.

The performed calculations show that the analysis of the transport properties of the active region of nanodevices cannot be conducted independently of the contacts, or otherwise the results can be overstated. This conclusion can be additionally enhanced by results presented in Refs. [61,62], where authors performed Monte Carlo simulations of Wigner wave packets scattered on static or dynamic potential barrier, simulating the effect of noncoherent scattering in contacts. Moreover, the nonequilibrium Green function method was applied to investigate the influence of some particular mechanisms, i.e., geometry of leads and doping on the transport characteristics of the nanodevice [41,63]. Our approach generalizes these results in some sense and entitles us to formulate a statement that if any scattering mechanisms exist, not defined explicitly but resulting in thermalization of electrons in contacts (in particular scattering on dopants), they damp the current-voltage characteristics by a factor related to the imaginary part of the self-energy. Such influence of the quality of contacts indicates necessity of further studies devoted to the

transport properties of nanodevices treated as open systems, most notably with detailed analysis of individual scattering mechanisms in contacts which may help to establish their contributions to the total thermalization of electrons.

Summarizing, we believe that the inflow boundary condition based on the proposed form of the equilibrium distribution function together with the given generalization can be applied in calculations of the transport properties of various nanosystems in different transport regimes, which are determined by the appropriate characteristic length-scale relationship (i.e., involving the coherence length, the effective wavelength, the mean free path and the lengths of the system and its active region), to make a substantial advance in the realistic description of the transport properties beyond the dissipationless Landauer formula.

ACKNOWLEDGMENTS

This work was supported by the Polish Ministry of Science and Higher Education and its grants for scientific research.

APPENDIX: SPECTRAL FUNCTION AND BOUNDARY CONDITION

It is generally accepted that the collisions of the conduction electrons with impurities, phonons, or other electrons in contacts leads to thermal equilibrium between the electrons and their surroundings [48]. Regardless, it is also known that the scattering of the electrons on impurities can modify an electron's interaction with phonons or electrons [64]. In these cases, the transfer of energy between the electron gas and the phonon gas due to an inelastic or quasielastic scattering has a statistical nature. As a consequence, spontaneous transitions between different energetic states of the electrons are observed in contacts. Theoretical description of these processes can be derived from the effective one-particle Hamiltonian in which the potential energy is represented by the self-energy, $\hat{\Sigma}$, i.e.,

$$\hat{H} = \hat{H}_0 + \hat{\Sigma}, \quad (\text{A1})$$

where \hat{H}_0 is the free-electron Hamiltonian. In principle, the self-energy is a complex function,

$$\hat{\Sigma} = \Re \hat{\Sigma} + i \Im \hat{\Sigma}, \quad (\text{A2})$$

where the matrix elements of the real part, $\Re \Sigma = \Sigma_R$, correspond to the effective shift and renormalization of the kinetic energy of the free electrons, whereas the matrix elements of the imaginary part, $\Im \Sigma = -\Gamma$, correspond to the finite lifetime of the momentum states due to the above-mentioned interactions. Therefore, it can be expressed by the relaxation time τ_Γ via the formula $\Gamma = \hbar/(2\tau_\Gamma)$, which stems from the Fermi golden rule and the Born approximation. On the other hand, the self-energy determines the analytic structure of the retarded Green function, which in turn can be used to determine the spectral function in the following way [51]:

$$A(k, E) = -2 \Im \frac{1}{E - E(k) - \Sigma(k, E)}. \quad (\text{A3})$$

In this case, the self-energy $\Sigma(k, E)$ is a complex function of momentum and energy, and its form can be determined from

the solution of the following self-consistent equation,

$$\Sigma(k, E) = \frac{n_I}{\Omega} \sum_{\mathbf{k}'} \frac{|M(k', k)|^2}{E - E(k') - \Sigma(k', E)}, \quad (\text{A4})$$

where $M(k', k)$ corresponds to the transition matrix element. Hence, we can conclude that the relaxation time defined by the imaginary part of the self-energy depends on the momentum and energy variables. However, we should point out that if the self-energy is a slowly varying function of momentum, then it can be replaced by its average value or it can be calculated in the first Born approximation.

The spectral function allows counting the number of states with energy E and momentum k participating in the thermalization due to the scattering process in contacts. Simple algebraic manipulations allow writing the spectral function in the form

$$A(k, E) \propto \frac{1}{\pi} \frac{\Gamma(k, E)}{[E - E(k) - \Sigma_R(k, E)]^2 + \Gamma^2(k, E)}, \quad (\text{A5})$$

which is a Lorentzian-type function peaked around $E = E(k) + \Sigma_R(k, E)$, with the width proportional to the imaginary part of the self-energy. We note that if the interactions are weak, then the self-energy is small, and the corresponding spectral function is more peaked. In turn, the absence of the interactions (the free electron model) leads to the Dirac-delta form of the spectral function. Inclusion of the interactions creates the possibility of modeling the spectral function by other functions that approach the Dirac delta. We have performed some additional calculations utilizing the Gaussian and the Voigt profile, but the results show that the impact of these changes on current-voltage characteristics is nearly the same as for the Lorentzian form of the spectral function. Further, the spectral function is related to the equilibrium distribution function

$$f_{\text{eq}}^{L(R)}(E(k)) = \int_0^\infty dE \delta_\Gamma(E - E(k)) f^{L(R)}(E) \quad (\text{A6})$$

via the fluctuation-dissipation theorem, namely [51,64]

$$-iG^<(k, E) = 2\pi A(k, E) f^{L(R)}(E), \quad (\text{A7})$$

where $f^{L(R)}(E)$ is the Fermi-Dirac distribution function for the free electrons in the contacts, and $G^<(k, E)$ is the lesser Green function. From Eq. (A7) results, the fluctuations at equilibrium due to the interactions with phonons or electrons in the presence of the impurities are related to the dissipation in the contacts. Based on these results, we can further conclude that the dissipation in contacts destroys the phase coherence of the injected conduction electrons, since the change of phase estimated from the uncertainty principle is equal $\Delta\varphi_\Gamma = \Delta E \tau_\Gamma/\hbar$, where ΔE results from the exchange of the energy between electrons and phonons systems. Moreover, in the Schrödinger's approach to quantum mechanics, the wave functions of the injected electrons, which are solutions of the Schrödinger equation with the complex potential, are not plane waves, but include an additional exponential damping factor which depends on Γ .

- [1] I. Knezevic, *Phys. Rev. B* **77**, 125301 (2008).
- [2] F. Dolcini, R. C. Iotti, and F. Rossi, *Phys. Rev. B* **88**, 115421 (2013).
- [3] E. Wigner, *Phys. Rev.* **40**, 749 (1932).
- [4] V. I. Tatarskiĭ, *Sov. Phys. Usp.* **26**, 311 (1983).
- [5] M. Hillery, R. F. O’Connell, M. O. Scully, and E. P. Wigner, *Phys. Rep.* **106**, 121 (1984).
- [6] H.-W. Lee, *Phys. Rep.* **259**, 147 (1995).
- [7] T. Curtright and C. Zachos, *Mod. Phys. Lett. A* **16**, 2381 (2001).
- [8] D. Querlioz and P. Dollfus, *The Wigner Monte-Carlo Method for Nanoelectronic Devices: A Particle Description of Quantum Transport and Decoherence* (ISTE Ltd. and John Wiley and Sons, Inc., New York, 2010).
- [9] Y. Shalibo, R. Resh, O. Fogel, D. Shwa, R. Bialczak, J. M. Martinis, and N. Katz, *Phys. Rev. Lett.* **110**, 100404 (2013).
- [10] O. Steuernagel, D. Kakofengitis, and G. Ritter, *Phys. Rev. Lett.* **110**, 030401 (2013).
- [11] S.-B. Zheng, Y.-P. Zhong, K. Xu, Q.-J. Wang, H. Wang, L.-T. Shen, C.-P. Yang, J. M. Martinis, A. N. Cleland, and S.-Y. Han, *Phys. Rev. Lett.* **115**, 260403 (2015).
- [12] M. Reboiro, O. Civitarese, and D. Tielas, *Phys. Scr.* **90**, 074028 (2015).
- [13] H. Zhu, *Phys. Rev. Lett.* **117**, 120404 (2016).
- [14] D. Kienzler, C. Flühmann, V. Negnevitsky, H.-Y. Lo, M. Marinelli, D. Nadlinger, and J. P. Home, *Phys. Rev. Lett.* **116**, 140402 (2016).
- [15] T. Tilma, M. J. Everitt, J. H. Samson, W. J. Munro, and K. Nemoto, *Phys. Rev. Lett.* **117**, 180401 (2016).
- [16] J. Schachenmayer, A. Pikovski, and A. M. Rey, *Phys. Rev. X* **5**, 011022 (2015).
- [17] D. Kakofengitis, M. Oliva, and O. Steuernagel, *Phys. Rev. A* **95**, 022127 (2017).
- [18] W. P. Schleich, *Quantum Optics in Phase Space* (John Wiley and Sons, Inc., New York, 2001).
- [19] W. H. Zurek, *Rev. Mod. Phys.* **75**, 715 (2003).
- [20] W. R. Frensley, *Rev. Mod. Phys.* **62**, 745 (1990).
- [21] M. Nedjalkov, S. Selberherr, D. Ferry, D. Vasilevska, P. Dollfus, D. Querlioz, I. Dimov, and P. Schwaha, *Ann. Phys.* **328**, 220 (2013).
- [22] R. P. Zaccaria and F. Rossi, *Phys. Rev. B* **67**, 113311 (2003).
- [23] R. Rosati, F. Dolcini, R. C. Iotti, and F. Rossi, *Phys. Rev. B* **88**, 035401 (2013).
- [24] I. Dimov, M. Nedjalkov, J. M. Sellier, and S. Selberherr, *J. Comput. Electron.* **14**, 859 (2015).
- [25] C. Jacoboni, A. Bertoni, P. Bordone, and R. Brunetti, *Math. Comput. Simulation* **55**, 67 (2001).
- [26] M. Nedjalkov, H. Kosina, S. Selberherr, C. Ringhofer, and D. K. Ferry, *Phys. Rev. B* **70**, 115319 (2004).
- [27] O. Muscato and W. Wagner, *SIAM J. Sci. Comput.* **38**, A1483 (2016).
- [28] D. Szydłowski, M. Wołoszyn, and B. J. Spisak, *Semicond. Sci. Technol.* **28**, 105022 (2013).
- [29] K.-Y. Kim, *J. Appl. Phys.* **102**, 113705 (2007).
- [30] A. S. Costolanski and C. T. Kelley, *IEEE Trans. Nanotechnol.* **9**, 708 (2010).
- [31] K.-Y. Kim and S. Kim, *Solid-State Electron.* **111**, 22 (2015).
- [32] D. Schulz and A. Mahmood, *IEEE J. Quant. Electronics* **52**, 1 (2016).
- [33] E. A. Gómez, S. P. Thirumuruganandham, and A. Santana, *Comput. Phys. Commun.* **185**, 136 (2014).
- [34] B. J. Spisak, M. Wołoszyn, and D. Szydłowski, *J. Comput. Electron.* **14**, 916 (2015).
- [35] R. Cabrera, D. I. Bondar, K. Jacobs, and H. A. Rabitz, *Phys. Rev. A* **92**, 042122 (2015).
- [36] A. Thomann and A. Borz, *Numer. Methods Partial Differential Equations* **33**, 62 (2017).
- [37] S. Hershfield, J. H. Davies, and J. W. Wilkins, *Phys. Rev. Lett.* **67**, 3720 (1991).
- [38] Y. Meir and N. S. Wingreen, *Phys. Rev. Lett.* **68**, 2512 (1992).
- [39] M. V. Fischetti, *J. Appl. Phys.* **83**, 270 (1998).
- [40] T. Schwamb, B. R. Burg, N. C. Schirmer, and D. Poulidakos, *Appl. Phys. Lett.* **92**, 243106 (2008).
- [41] Y. He, Y. Wang, G. Klimeck, and T. Kubis, *Appl. Phys. Lett.* **105**, 213502 (2014).
- [42] W. Lu and J. Xiang (eds.), *Semiconductor Nanowires* (The Royal Society of Chemistry, Cambridge, 2015).
- [43] R. Songmuang, G. Katsaros, E. Monroy, P. Spathis, C. Bougerol, M. Mongillo, and S. De Franceschi, *Nano Lett.* **10**, 3545 (2010).
- [44] E. E. Boyd, K. Storm, L. Samuelson, and R. M. Westervelt, *Nanotechnology* **22**, 185201 (2011).
- [45] Y. Shao, S. D. Carnevale, A. T. M. G. Sarwar, R. C. Myers, and W. Lu, *J. Vac. Sci. Technol. B* **31**, 06FA03 (2013).
- [46] S. Barraud, *J. Appl. Phys.* **110**, 093710 (2011).
- [47] M. Wołoszyn, B. J. Spisak, J. Adamowski, and P. Wójcik, *J. Phys.: Condens. Matter* **26**, 325301 (2014).
- [48] N. W. Ashcroft and N. D. Mermin, *Solid State Physics* (Holt Rinehart and Winston, New York, 1976).
- [49] D. Taj, L. Genovese, and F. Rossi, *Europhys. Lett.* **74**, 1060 (2006).
- [50] S. Ho and K. Yamaguchi, *Semicond. Sci. Technol.* **7**, B430 (1992).
- [51] G. D. Mahan, *Many Particle Physics* (Kluwer Academic Plenum Publishers, New York, 2000).
- [52] A. Wacker, *Phys. Rep.* **357**, 1 (2002).
- [53] L. L. Bonilla and H. T. Grahn, *Rep. Prog. Phys.* **68**, 577 (2005).
- [54] O. Jonasson and I. Knezevic, *J. Comput. Electron.* **14**, 879 (2015).
- [55] C. Gutsche, A. Lysov, I. Regolin, K. Blekker, W. Prost, and F. J. Tegude, *Nanoscale Res. Lett.* **6**, 65 (2010).
- [56] H. Mizuta and T. Tanoue, *The Physics and Applications of Resonant Tunnelling Diodes* (Cambridge University Press, Cambridge, 2006).
- [57] S. Datta, *Quantum Transport: Atom to Transistor* (Cambridge University Press, Cambridge, 2005).
- [58] The current I_c corresponds to the first moment of the WDF, which is determined by the solution of the Wigner kinetic equation without the scattering integral and with the boundary conditions given by the bare Fermi-Dirac function.
- [59] P. Mazumder, S. Kulkarni, M. Bhattacharya, J. P. Sun, and G. I. Haddad, *Proc. IEEE* **86**, 664 (1998).
- [60] N. A. Bruce and G. J. Morgan, *Phys. Rev. B* **51**, 12313 (1995).
- [61] A. Bertoni, P. Bordone, and G. Ferrari, *J. Comput. Electron.* **2**, 137 (2003).
- [62] G. Ferrari, P. Bordone, and C. Jacoboni, *Phys. Lett. A* **356**, 371 (2006).
- [63] S. Berrada, M. Bescond, N. Cavassilas, L. Raymond, and M. Lannoo, *Appl. Phys. Lett.* **107**, 153508 (2015).
- [64] J. Rammer, *Quantum Field Theory of Non-equilibrium States* (Cambridge University Press, Cambridge, 2007).